HYDROLOGICAL PROCESSES
Hydrol. Process. (2011)
Published online in Wiley Online Library
(wileyonlinelibrary.com) DOI: 10.1002/hyp.7843

Hydrological and hydrochemical processes observed during a large-scale infiltration experiment at the Super-Sauze mudslide (France)

T.-H. Debieche,[1,2] T. A. Bogaard,[3] V. Marc,[1]* C. Emblanch,[1] D. M. Krzeminska[3] and J.-P. Malet[4]

[1] *EMMAH, UMR 1114 INRA-UAPV, Université d'Avignon et des Pays de Vaucluse, 33 rue Louis Pasteur, F-84000 Avignon, France*
[2] *Water and Environmental Team, Geological Engineering Laboratory, Jijel University, PO Box 98, 18000 Jijel, Algeria*
[3] *Water Resources Section, Faculty of Civil Engineering and Geosciences, Delft University of Technology, Stevinweg 1, NL-2628 CN Delft, The Netherlands*
[4] *IPGS, Université de Strasbourg/EOST, CNRS, 5 rue Descartes, F-67084 Strasbourg, France*

Abstract:

Rainfall is one of the major triggering factors of landslides, and its pattern controls their temporal behaviour. Characterization of the groundwater processes and possible preferential infiltration of rainfall is necessary, challenging and very relevant for landslide hazard analysis. The objective of this paper is to identify the groundwater dynamics (matrix flow and preferential flow) within highly heterogeneous and fissured reworked black marl material, using a large-scale infiltration test. The artificial rainfall experiment over a 100 m^2 infiltration plot monitored with several hydrological, hydrochemical and geophysical equipments was carried out on the Super-Sauze mudslide (South French Alps). High resolution groundwater and water quality measurements were collected. Artificial rainfall was applied over a period of 14 days. Conservative tracers (Br^- and Cl^-) were used successively during the infiltration period. The mean rainfall intensity was 8·5 mm h^{-1} with a mean tracer concentration of 100 mg l^{-1}. The hydrodynamic and hydrochemical responses of the tracing experiments allowed us to get a new insight into: (1) the horizontal and vertical variability of the rain infiltration in unstable black marl hillslopes; (2) the effect of shallow fissuration on the groundwater recharge; (3) the role of piston flow on the rate of water level changes and the increase of pore water pressures and (4) the effect of material heterogeneity in the development of preferential water flows and local perched water tables. Copyright © 2011 John Wiley & Sons, Ltd.

KEY WORDS mudslide; black marls; hydrochemistry; tracing experiment; preferential flow; heterogeneity

Received 21 July 2009; Accepted 19 July 2010

INTRODUCTION

What is the impact of infiltration conditions and subsurface flow processes (preferential vertical flow, interaction with matrix flow) upon slope stability? In most mountainous areas, the answer to this question is of primary importance to improve landslide hazard forecast. Because of their swiftness, of the possible fluidization pattern and of the large mass involved, mudslides are one of the most dangerous natural disasters. Their occurrence is a function of factors such as slope angle, geometry of the mobilized mass, soil strength and pore water pressure. All these factors are relatively stable in time except for water pressure and partial saturation, which are related to the rainfall infiltration and can change rapidly. The increase of pore water pressure and partial saturation decreases the effective stresses in the soil and thus affect slope stability.

In a homogeneous medium, water flow can be described by the Richard's equation for both saturated and unsaturated conditions. However, in a heterogeneous soil, there is no generally accepted equation to simulate the water flow. This is mainly due to difficulties arising in describing the interactions between the flow processes in different domains. Several approaches have been proposed such as dual-porosity (van Genuchten and Wierenga, 1976), dual-permeability (Pruess and Wang, 1987; Gerke and van Genuchten, 1993; Jarvis, 1994), multi-porosity and/or multi-permeability models (Gwo *et al.*, 1995; Hutson and Wagenet, 1995). The results obtained with these approaches show good results as long as the soil has a relatively low degree of heterogeneity and as a good knowledge of the spatial distribution of the heterogeneity exists. In mudslides, the soil shows abundant small and large scale heterogeneities which also evolve in the course of the time. Fissures may open or close depending on the deformation rates which results in changes over time of the permeabilty. Obviously, to describe the hydrodynamics in such a medium is a tough job. However, this heterogeneity is of major importance on the water flow in the mudslides. Two major aspects of the influence of soil heterogeneity will be discussed in this work: the influence of preferential flow paths and the influence of local perched water bodies.

Preferential flow paths are of two types: (1) bypass flow, through macropores and fissures (active when the inflow rate exceeds the infiltration rate of the soil matrix) and (2) fingered flow, linked to the high non-linearity

* Correspondence to: V. Marc, EMMAH, UMR 1114 INRA-UAPV, Université d'Avignon et des Pays de Vaucluse, 33 rue Louis Pasteur, 84000 Avignon, France. E-mail: vincent.marc@univ-avignon.fr

Copyright © 2011 John Wiley & Sons, Ltd.

of unsaturated flow processes even for macroscopically homogeneous soils (Liu *et al.*, 2005). Consequently, two roles of preferential flow paths in mudslides can be observed. On the one hand, preferential flow paths give rapid access to the groundwater system, shortening the response time of triggering events and increasing the frequency of failures; on the other hand, they ease the drainage of the groundwater body within the matrix during dry periods and limits pore water pressures, which may reduce the extent of potential unstable areas within a slope (McDonnell, 1990; Uchida *et al.*, 2001; Uchida, 2004). Furthermore, the heterogeneous character of a mudslide facilitates the development of perched water bodies or even perched aquifers, often in the topsoil layers. This plays an important role in (1) superficial slope stability (e.g. soil slips) and (2) the amount of water that refills the deeper groundwater table, thus influencing slope stability on a larger spatial and vertical scale.

A better understanding of the influence of soil heterogeneity on the hydrodynamics of mudslides requires on-site investigations. Environmental tracing (Bogaard *et al.*, 2004; Kabeya *et al.*, 2007; Viville *et al.*, 2007; Cras *et al.*, 2007) or artificial tracing (Einsiedl, 2005; Mali *et al.*, 2007) combined to hydrological surveys are among the most convenient investigation methods to characterize the subsurface flow, as the hydrodynamic and hydrochemical responses contain information on the water pathways. Artificial tracing is often carried out at the laboratory scale (Allaire-Leung *et al.*, 2000; Allaire *et al.*, 2002; Larsbo and Jarvis, 2006) or with lysimeters (Stumpp *et al.*, 2007). Plot scale artificial tracing of subsurface water flow is seldom studied owing to investigation difficulties in the field (Hirotaka *et al.*, 2004; Binet *et al.*, 2006).

This paper presents the results of an experimental investigation carried out on a large plot (100 m^2) located on the Super-Sauze mudslide. The Super-Sauze mudslide is a typical example of mass movement developed in the black marl outcrops of the South French Alps (Lacube and Durville, 1989; Malet *et al.*, 2005a,b). Water flow conditions in the Super-Sauze mudslide have previously been investigated from various experimental approaches (Malet *et al.*, 2003; Grandjean *et al.*, 2006; De Montety *et al.*, 2007). A first modelling exercise has been proposed by Malet *et al.* (2005b) with a conceptual 1-D description of rapid infiltration. The present experiment consists in applying bromide- and chlorite-enriched artificial rainfall during two periods of 3 days. Multi-point hydrological and hydrochemical monitoring has been carried out throughout the experiments.

The present paper aims at unravelling the hydrodynamic and hydrochemical response to rainfall forcing with the use of a large-scale tracing experiment and specifically to (1) determine the horizontal and vertical pattern of water infiltration in the mudslide; (2) characterize the groundwater behaviour and the flow distribution as a function of soil heterogeneity and (3) generalize the above observations in a conceptual model describing the hydrodynamic behaviour of the mudslide.

EXPERIMENTAL SITE

The Super-Sauze mudslide is located in the south-east French Alps (Alpes-de-Haute-Provence). The elevation ranges from 1740 to 2105 m, the average slope is of 25° and the area stretches roughly over 11 ha (825 m long and 135 m wide on average; Figure 1a). Callovian-Oxfordian black marls constitute most of the geology formations. The movement of the mudslide ranges from 0·01 to 0·40 m day^{-1} (Malet *et al.*, 2005a). The groundwater originates mostly from rainfall infiltration and to a certain extent from deep water sources along major faults (De Montety *et al.*, 2007). One spring (Goutta) spurts above the mudslide (Figure 1a) in a moraine formation.

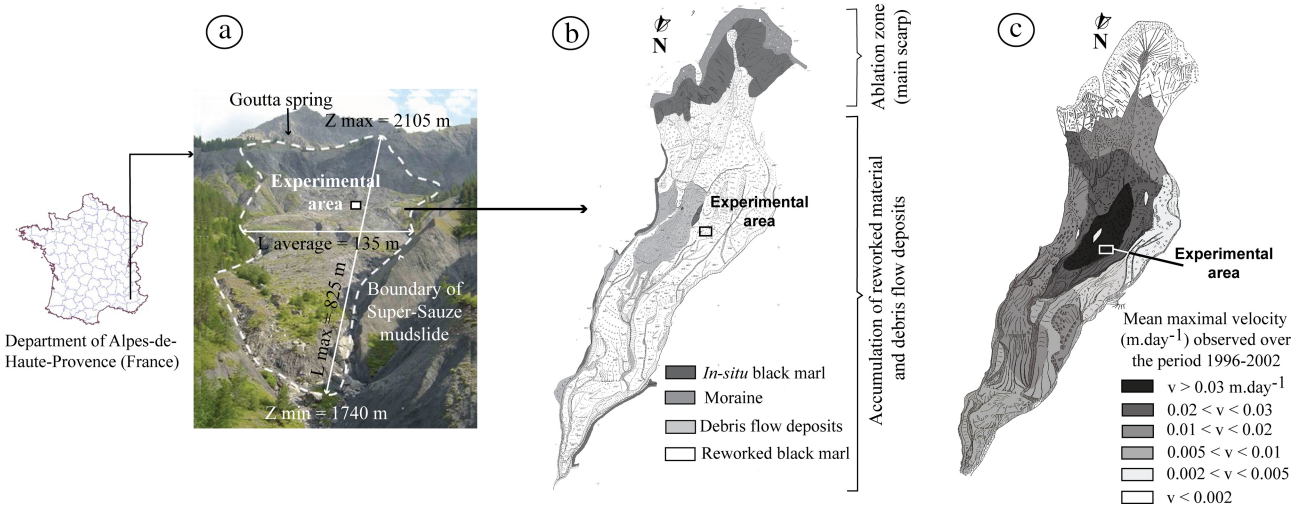

Figure 1. Overview of the experimental plot. (a) Picture of Super-Sauze mudslide, (b) Geology of the mudslide (Malet, 2003), (c) Mean maximal velocity of the mudslide observed during the period 1996–2002 (Malet, 2003)

Copyright © 2011 John Wiley & Sons, Ltd.

The experimental plot (14×7 m^2) is located in reworked black marls in the most active part of the mudslide (Figure 1). The average slope of the plot is of 20°. The mean maximal displacement velocity varies between 0·02 and 0·03 m day^{-1} (Travelletti *et al.*, 2008). The bedrock lays at 7 m of depth and is assumed to be homogeneous. The mudslide materials consist of a silty-sand matrix mixed with moraine debris. They are highly heterogeneous owing to the different levels of marl alteration and the mixing induced by mass movement processes along the slope (Malet, 2003). Permeabilty of the matrix varies greatly because of the variety of secondary mass movement processes influencing the material distribution, such as mudslide accumulation lobes or local wash deposits. Wrapped within the matrix, unweathered marly blocks may also produce local hydraulic barriers (laterally or vertically; Malet *et al.*, 2003).

The morphological pattern of the experimental plot can be split in two parts (Figure 2): the eastern side, where some fissures appear at the surface, and the western side where the surface seems not influenced by fissures. All the fissures of the infiltration area are characterized by their length (0·1–1 m), depth (0·05–0·25 m), and the distance between the fissures (0·05–0·50 m). In the upper part, all the fissures have an E–W orientation, but in the downslope part only one fissure is visible and it has a N–S orientation.

EQUIPMENT AND METHODS

The tracing infiltration experiment was conducted with two tracers (Cl^- and Br^-) and over two periods of 3 days: the first (10–13 July 2007) with a mean rainfall intensity of 8 mm h^{-1} and 90 mg l^{-1} of bromide concentration; the second (17–20 July 2007) with a mean rainfall intensity of 9 mm h^{-1} and 100 mg l^{-1} of chloride concentration, and in between 4 days of rest to allow most of water to drain or evaporate. The equipment and the hydrological and hydrochemical monitoring set-up are presented in Figure 2.

The average annual rainfall in Barcelonnette (5 km from Super-Sauze landslide) over the period 1994 and 2002 is of 790 mm and the annual average hourly intensity of a rain event is 12 mm h^{-1} (Malet, 2003). This value of the intensity rainfall slightly outstrips the artificial rainfall intensity.

- *Rainfall observations:* six rotary sprinklers were used to apply the artificial rainfall. They were located all around the experimental plot and spaced out 7 m apart. The water used for the tracing experiment was taken from the Goutta spring (Figure 1) because of its low degree of mineralization (higher electric conductivity than that of rainwater mostly due to greater bicarbonate content) (Table I). The water towards the experimental plot ran through flexible water tubes and

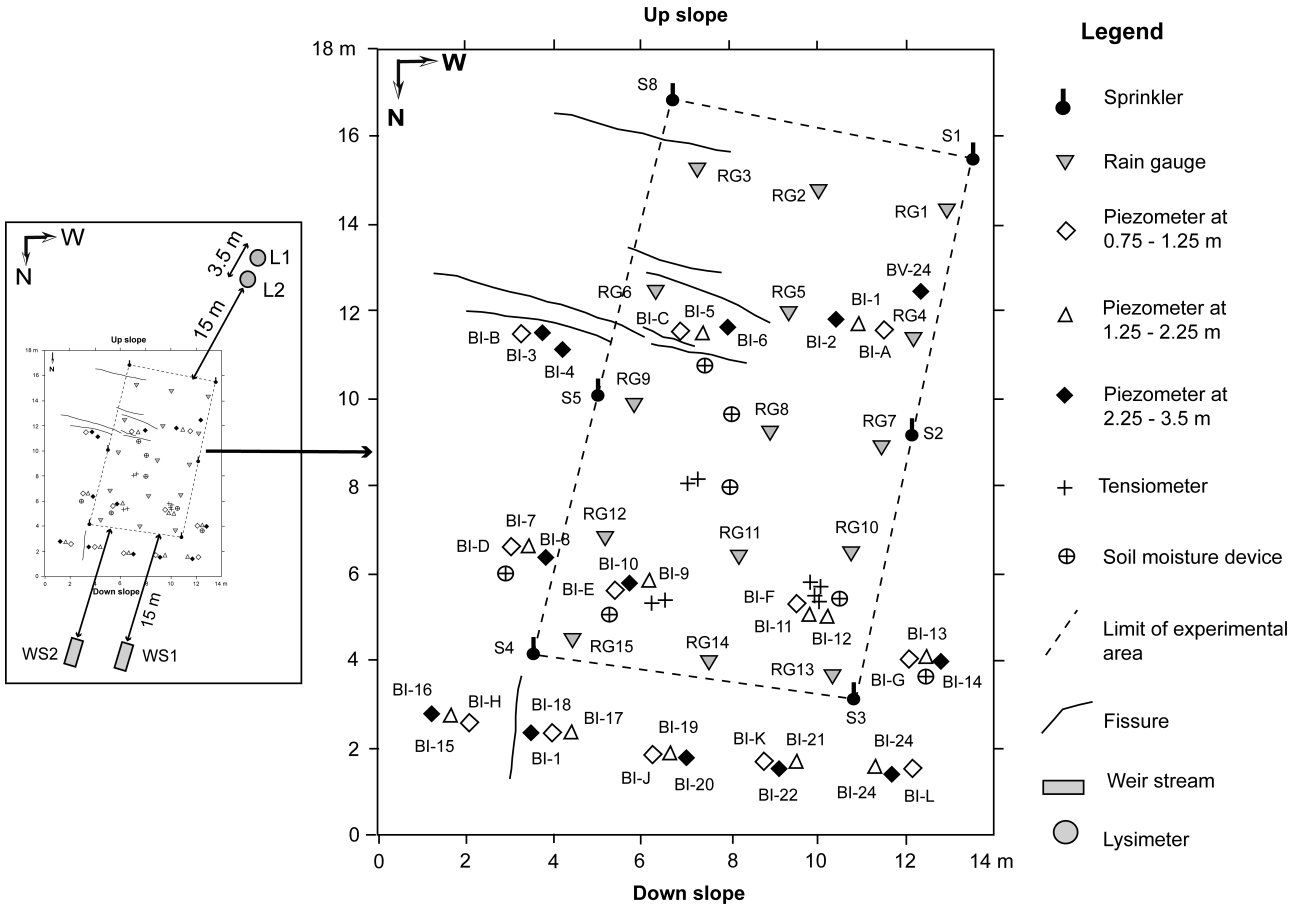

Figure 2. Monitoring set-up in the experimental plot

Copyright © 2011 John Wiley & Sons, Ltd.

Copyright © 2011 John Wiley & Sons, Ltd.

Table I. Chemical composition of water from the experimental plot, the mudslide, the spring water and the natural rainfall before the experiment

Location	Statistic	T (°C)	pH	Cond. (25 °C) (µS cm^{-1})	Eh (H) (mV)	HCO_3^- (mg l^{-1})	Cl^- (mg l^{-1})	NO_3^- (mg l^{-1})	SO_4^{2-} (mg l^{-1})	Br^- (mg l^{-1})	Na^+ (mg l^{-1})	K^+ (mg.l^{-1})	Ca^{2+} (mg.l^{-1})	Mg^{2+} (mg.l^{-1})
Mudslide (20 May 2003–18 October 2006) 160 samples for 38 piezometers)	Maximum	22·4	8·6	6960	502	640	33·5	19·7	4106	0·0	1083	34·7	604	491
	Average	10·0	7·5	2650	306	268	2·9	2·8	1621	0·0	150	10·0	238	196
	Minimum	2·2	7·0	140	48	58	0·2	0·1	12	0·0	0·8	0·4	37	7
Goutta source (17 July 2007; 19 h) 1 sample	Concentration	6·7	8·0	238	440	117	0·2	0·6	17	0·0	0·9	0·9	28	5
Natural rainfall (2 samples)	Concentration (average)	—	—	—	—	—	0·5	—	3	—	0·4	0·1	5·3	0·3
Experimental area (10 July 2007; 13–14 h) 13 samples for 13 piezometrs)	Maximum	15·9	7·9	5590	482	337	17·0	4·6	2546	0·0	449	62·6	409	326
	Average	13·9	7·5	3397	458	280	6·2	2·3	1943	0·0	261	18·2	271	212
	Minimum	12·5	7·1	1227	439	234	1·1	0·3	566	0·0	63	6·2	90	63

As not all piezometers had water, the number of piezometers where sample could be collected is smaller than the total number of piezometers.

blended with tracer in a 5 m^3 water tank. A cumulative water-meter controlled the input volume. Hereafter, the water was stored in two basins, from where it was pumped and transferred to the sprinklers with 1·5–2 bars of pressure.

Fifteen rain gauges (maximum depth 30 mm) were used to control the rainfall depth and areal distribution. They were placed at 3 m regular intervals over the experimental plot. The rainfall depths were hand-recorded at variable time steps (1–3 h).

- *Evaporation observations:* two types of lysimeter measurements were performed to determine the soil evaporation; constant head (Aboukhaled *et al*., 1982) and micro-lysimeters (Boast and Robertson, 1982). Two *in-situ*, constant head lysimeters were made of polyvinyl chloride (PVC) tubes (15 cm inner diameter, 50 cm length) to measure soil evaporation. The constant head lysimeters, kept nearby saturation (water level at 10 and 25 cm below surface), estimated the maximum soil evaporation during the experiment. The microlysimeters consisted of standard Kopecky rings of 100 cm^3 (Javaux and Vanclooster, 2006). They were used to determine the actual soil evaporation by weight difference over a 24-h period. These lysimeters were installed at around 15 m from the infiltration plot. The evaporation measurements were carried out every day.
- *Run-off observations:* two weirs (Neyrpik Alsthom trademark—type A) were used to measure the overland flow. They were set up 15 m downstream of the experimental plot. The overland flow was sampled 24 times over the period 11–13 and 19 July 2007 and a total of 30 manual discharge measurements of the overland flow were carried out over the period 17–19 July 2007.
- *Hydrological observations in the unsaturated zone:* the experimental plot was equipped with: (1) sixteen soil moisture devices consisting in seven Time Domain Reflectometry (TDR) probes (Campbell Scientific CS 616 and CS 615), four WaterMark sensors (257 series) and five theta tubes (PR1/6 w-02) to measure the vertical soil moisture profile at 0·1, 0·2, 0·3, 0·4, 0·6 and 1·0 m depth; and (2) eight water tension sensors (4 UMS T4 (serial 813) and 4 SDEC). The soil water content and water pressure was monitored with a sampling rate of 1 min over the whole period of the experiment (13–24 July 2007).
- *Hydrological observations in the saturated zone:* A total of 37 open standpipe piezometers were installed at different depths (12 piezometers at depths of 0·75–1·25 m (noted BI-letter), 12 at depths of 1·25–2·25 m (noted BI-odd number except piezometer BI-12) and 13 at depths of 2·25–3·50 m (noted BI-even number). The annular spaces surrounding the piezometer screens were filled with sand/gravel pack over the height of 0·5, 1·0 and 1·0 m, respectively. On top of that, a bentonite seal was added over a height of 0·25, 0·50 and 0·50 m, respectively and finally soil was backfilled. The piezometers were nested in trinomes at different depths to study the vertical hydrodynamics. Thirteen of these piezometers were equipped with automatic recording water pressure devices (Diver, Keller and Paratronic sensors) with a recording rate of 1 min.
- *Physico-chemical measurements and chemical analyses:* A total of 1300 samples were collected during the experiment. Several physico-chemical parameters were measured *in-situ* (temperature, pH, EC and Eh using pH/Cond 340i/set -WTW- and redox -Ag/AgCl-probes). A total of 330 samples were analysed for major cations content (Ca^{2+}, Mg^{2+}, Na^{+}, K^{+}) using atomic absorption spectrometry (Spectr AA-640, Varian) and 1130 for anions concentration (Cl^{-}, Br^{-}, NO_3^{-}, SO_4^{2-}) using HPLC (high performance liquid chromatography, Dionex DX-120).

During both rainfall periods, the water was sampled every 1 h in piezometers BI-J, BI-19 and BI-20, every 3 h in piezometers BI-C, BI-E, BI-6, BI-9 and BI-10 and every 6 h in the remaining piezometers. During the in-between period and after the second rainfall period (20–23 July 2007), the sampling rate was of one sample per day for all piezometers.

The applied rain water was measured directly in the two reservoirs for the physico-chemical composition after each filling of the reservoir (the time step was typically 1 h). Water samples were stored in the field in an isolated box kept in a shaded area and afterwards at the laboratory in an air-conditioned room (19 °C).

Figure 3 summarizes the hydrological and hydrodynamic monitoring and sampling of the water during and after the experiment.

- *Permeability measurements:* the permeability of the topsoil of the experimental plot was determined by the Slug-test method (Bouwer and Rice, 1976). Several tests were realized in nine piezometers: two (BI-A and BI-C) at 1 m deep; two others (BI-1 and BI-9) at 1·5 and 2 m deep, respectively and five (BI-6, BI-8, BI-18 and BI-20) at 3 m deep.

RESULTS AND DISCUSSION

Hydrodynamic variations

Figure 4 summarizes the temporal and spatial pattern of the groundwater levels of all the piezometers which were equipped with dataloggers compared to the initial water levels.

In Figure 4a, three types of hydrological response can be distinguished:

- Attenuated input–output (Figure 4a-A): this behaviour shows a progressive increase of water level at the beginning of the experiment with a slow decrease afterwards. The water level slowly returns to its initial level but often remains slighthy above it. This is

Copyright © 2011 John Wiley & Sons, Ltd.

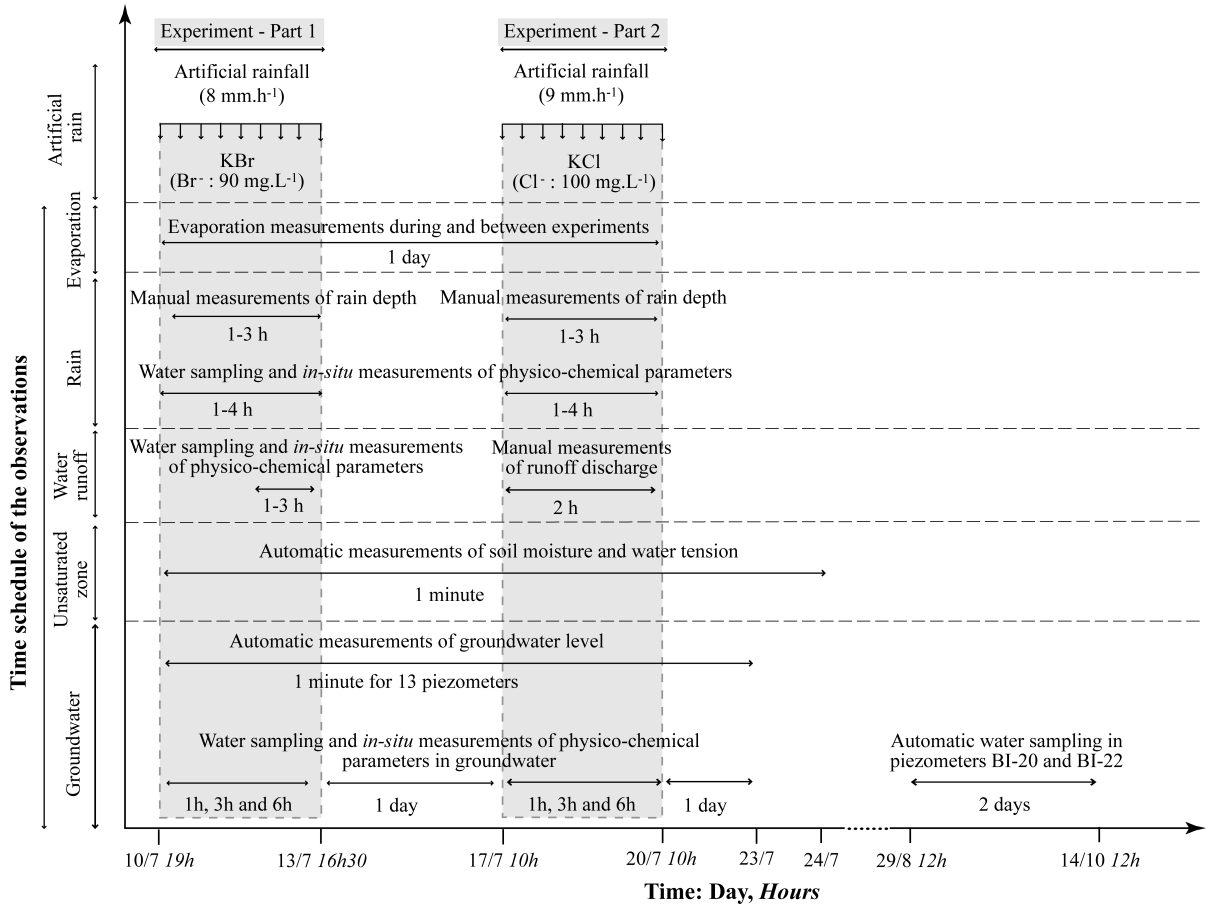

Figure 3. Overview of the experimental monitoring

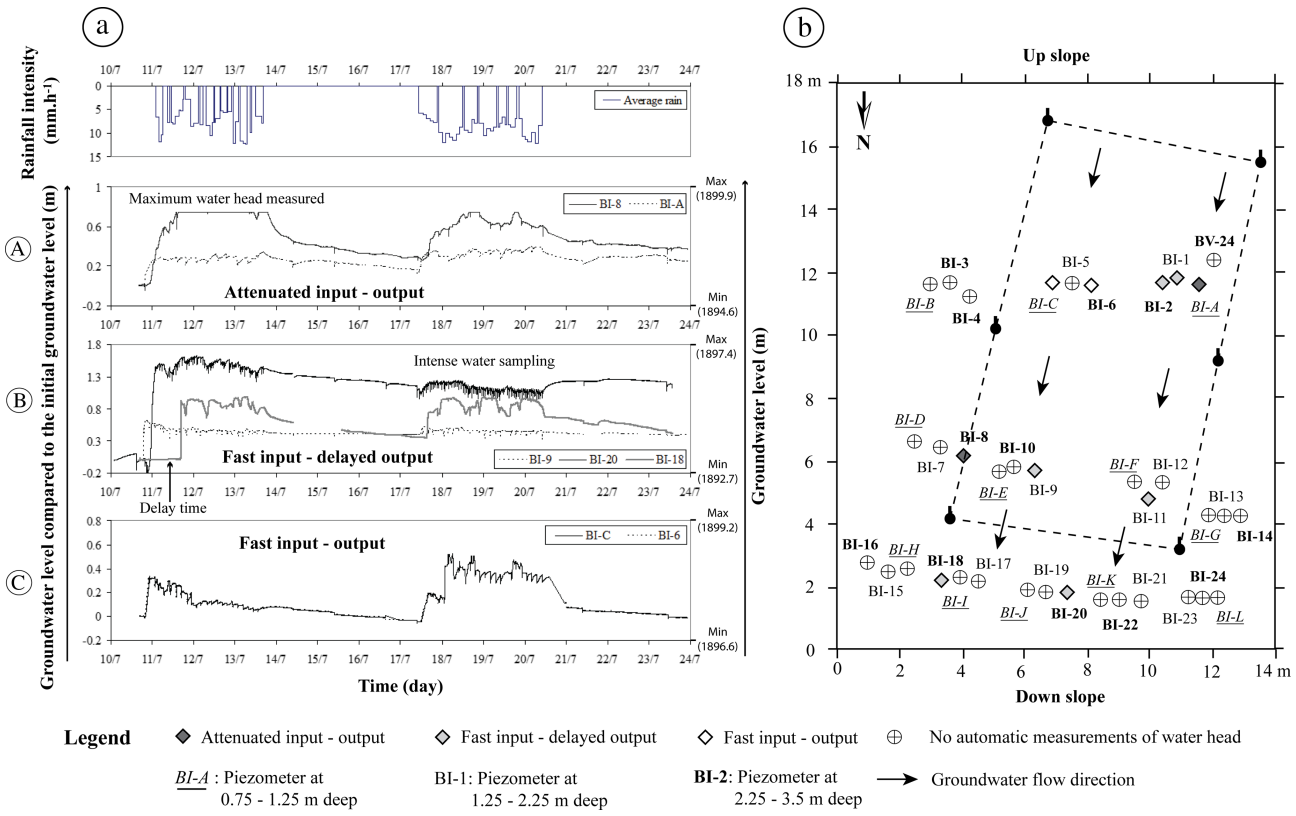

Figure 4. Temporal and spatial hydrodynamic behaviour of the experimental plot. (a) Temporal hydrodynamic behaviour; (b) Spatial hydrodynamic behaviour

Copyright © 2011 John Wiley & Sons, Ltd.

interpreted as matrix flow with a relatively low lateral permeability compared to the vertical permeability;

- Fast input, delayed output (Figure 4a-B): a steep rise of the water level at start. After the experiment, the water level does not return to its initial level. This indicates easy infiltration via preferential flow paths in the matrix but once filled they cannot drain rapidly. Piezometer BI-9 demonstrates such type of behaviour as it shows a fast reaction at the beginning of the experiment but the level does not drop in the dry period. During the second test, this piezometer shows a very limited reaction. These areas basically store the water for a certain period and only release it very slowly;
- Fast input–output (Figure 4a-C): a very fast response to rainfall as well as sudden water level drop after rainfall ceases. The water level then returns to its initial level. This is representative of a well-connected fissure system.

These observations lead to the following interpretation of the role of preferential flow. First, in case of fast input-delayed output, the secondary porosity of macropores and fissures increases the infiltration capacity of the soil and can facilitate infiltration into the matrix but as doing so, it increases interstitial pore water pressure. Second, in case of fast input–output system, the fissures rapidly drain the rain water. As a result, the interstitial pore water pressure decreases.

The distribution of the different types of hydrological responses (Figure 4b) shows no direct relation with:

- the surface fissures (Figure 2). Preferential flow can occur in the area with or without fissures visible at the surface (BI-9 and BI-20).
- the rainfall variability (Figure 5): the six sprinklers were positioned as such to ensure an even distribution of rain over the entire experimental plot and minimize overlap. Nevertheless, a large variability was observed between minimum and average rain (−40%) and between average and maximum rain (70%). Most of the piezometers are located between the rainfall intensity contours of 7 and 11 mm h^{-1} (Figure 5). This areal rainfall variability seems to have minor impact on the hydrological dynamics in the subsurface. The hydrodynamic reaction observed in the piezometers was not related to the rainfall distribution. Piezometers BI-1, BI-9 and BI-11 (1·5, 2·0 and 2·0 m deep, respectively) are located in the area with different average intensity (7·8, 9·0 and 10·9 mm h^{-1}, respectively) and show the same hydrodynamic reaction. On the contrary, piezometers BI-2 and BI-6 (3·45 and 3·00 m deep, respectively) are positioned in an area with nearly the same rain intensity (9·2 and 9·5 mm h^{-1}) and show quite different hydrodynamic reactions (high and low, respectively).

The rainfall variation during the experiment (11–20 July 2007) in the whole experimental area averaged

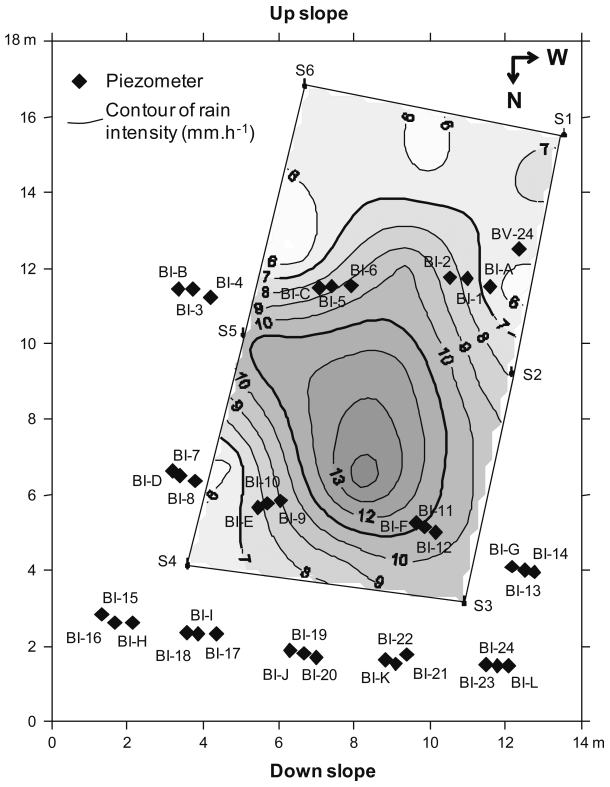

Figure 5. Spatial distribution of the average artificial rainfall

1·8 mm h^{-1}. The water level development showed that these input variations together with the discrete sampling of water for hydrochemical analysis resulted only in a noisy hydrodynamic signal. These short-term variations in water level banned getting a smoothed response but had no consequence on the general trend of the groundwater variation.

Figure 6 shows in detail the different hydrological responses with depth during the experiment:

- in the south-west corner, two piezometers (BI-A and BI-1) located at 1·0 and 1·5 m depth showed comparable responses to the rainfall input, whereas an attenuated response was observed for BI-2 at 3·5 m depth. A 1·0–1·4 m water level difference before, during and after the rainfall experiment was recorded between the BI-A and BI-2 which have their screens on 0·5–1·0 m and 2·5–3·5 m, respectively. Very high hydraulic gradients were observed between distant piezometers at different depths (for example 50° between BI-C and BI-8 which is much more than the surface slope). But for same depth piezometers (deep piezometers BI-2 and BI-8 or shallow piezometers BI-1 and BI-11), the hydraulic gradient (15·6° and 20·0°, respectively) was lower than or equal to the ground slope (20°).
- the piezometers BI-C and BI-6 which were located in the south-east corner at 1·0 and 3·0 m depth, respectively showed a 1·5–1·6 m head difference, but they recorded the same temporal behaviour. Clearly, the two systems cannot be connected to each other as they should have had the same water level. However, their reaction to the rainfall input was

Copyright © 2011 John Wiley & Sons, Ltd.

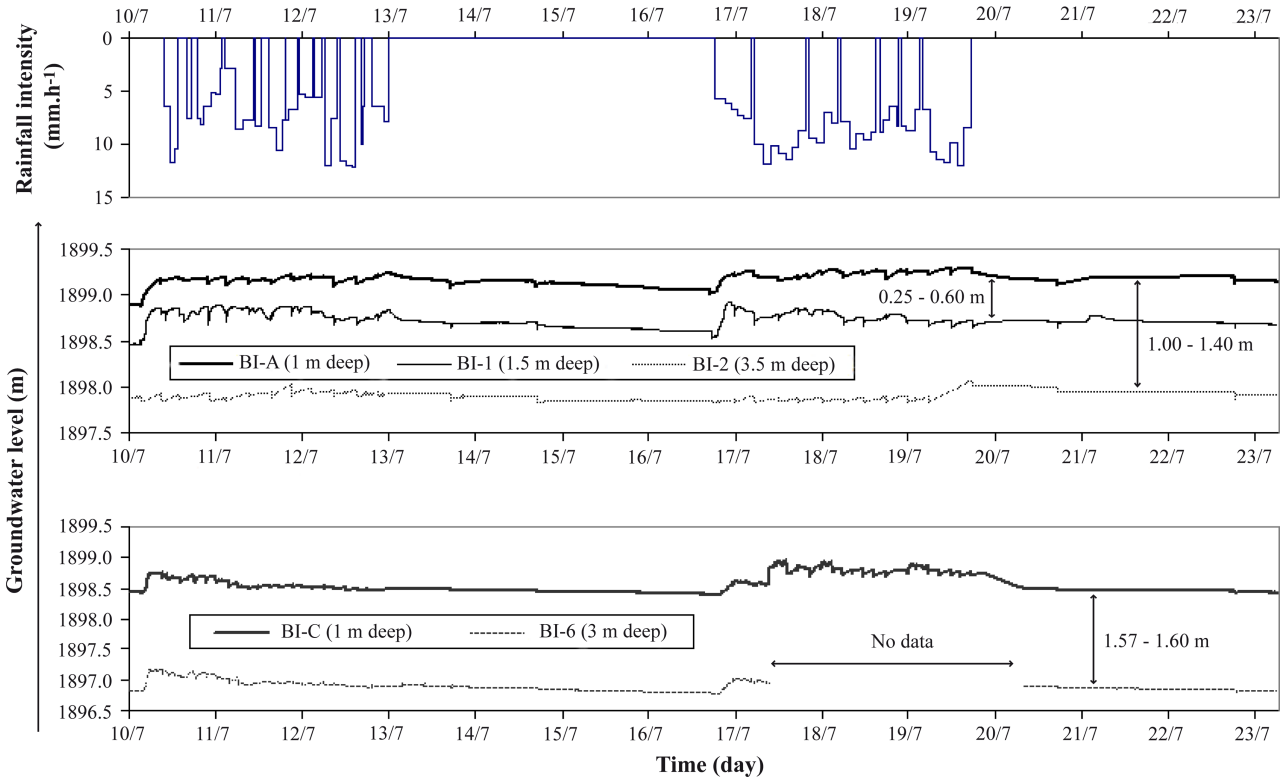

Figure 6. Groundwater level evolution of the piezometers at different depths

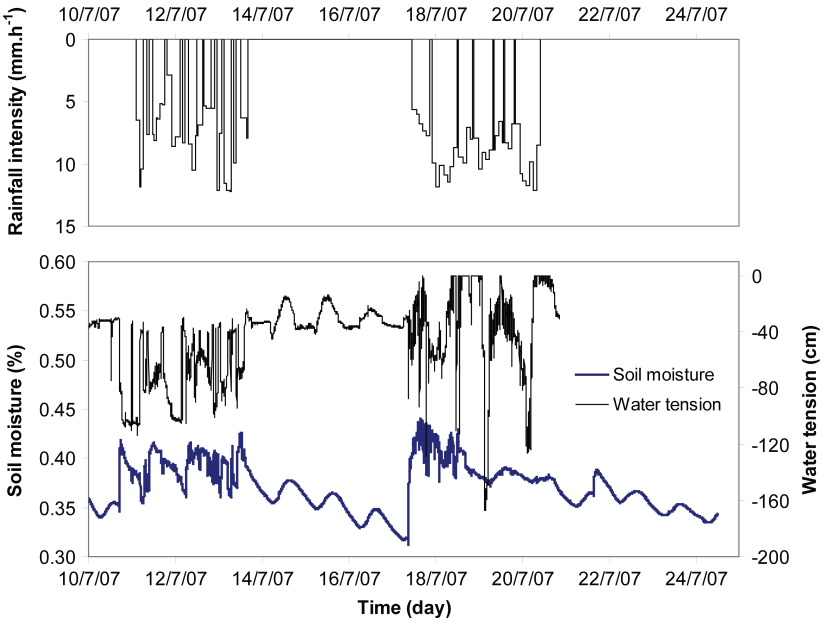

Figure 7. Water tension and soil moisture changes in the experimental area

similar. This will further be investigated with the use of tracers.

These observations prove the existence of several perched water bodies in the mudslide. This has two possible consequences for the triggering of movement within the mudslide. It decreases the rainfall infiltration and percolation towards the deeper groundwater and thus the possibility of global landslide acceleration; at the same time, it increases the water level close to the subsurface which could result in local shallow soil slips.

The monitoring network in the unsaturated zone gave limited insight. This is basically due to technical problems with several of the devices, to the lack of calibration curve due to missing temperature data (Watermark devices) or also to the fact that the soil around the devices was saturated. Only tensiometer T10 (located near the piezometers BI-E,9,10) gave some results although being affected by temperature influence (Figure 7). Among the

Copyright © 2011 John Wiley & Sons, Ltd.

soil moisture measurement devices only the TDR CS 616-4 (located in the centre of experimental area and at 0·15–0·45 m depth (Figure 7)) could be used, although it could not be calibrated against a field specific calibration. Figure 7 shows a rapid increase of soil moisture content and decrease of water tension after the start of the artificial rainfall, indicating a fast infiltration into the soil.

Hydrochemical changes

Initial hydrochemical conditions before the experiment. Table I gives the chemical composition of the groundwater at the experimental plot, the mudslide area, the Goutta spring and of the natural rainfall.

The chemical composition of the groundwater is characterized by a large range of electrical conductivity (140–7000 µs cm^{-1}) and by three dominant elements: sulphate (average 1621 mg l^{-1}), bicarbonate (average 268 mg l^{-1}) and calcium (average 238 mg l^{-1}). The Goutta spring water has a low conductivity (238 µs cm^{-1}) and only contains as dominant elements: bicarbonate (117 mg l^{-1}) and calcium (28 mg l^{-1}). This difference in water quality allows monitoring the artificial rain infiltration and its circulation in the subsurface.

General evolution of the characteristic elements during the experimentation. Three elements were selected to monitor the hydrochemical changes of the groundwater during the experiment:

- Cl^- and Br^- to trace the artificial rainwater, because these anions are absent (Br^-) or have a very low concentration (Cl^-, 0–33 mg l^{-1}) in the groundwater. Anion tracers are not subject to adsorbtion and ion exchange with clayey soils as clay minerals are also negatively charged. Nevertheless, they might not be perfect conservative tracers as they do not behave like water molecules, because of anion exclusion which accelerates the anion transport (Schoen *et al*., 1999a,b). This mechanism may result in a slight overestimation of the groundwater recharge dynamics.
- SO_4^{2-} to trace the natural groundwater, because this anion is abundant in the groundwater system and only present in low concentrations (17 mg l^{-1}) in the Goutta source.

The Br^-, Cl^- and SO_4^{2-} concentration time series during the experiment indicate three types of response (Figure 8):

- a high response in piezometers BI-C, J, 2, 9, 11, 17, 20 showing a sharp increase in bromide and chloride (up to 60–120 mg l^{-1}) concentrations, and rapid drop of sulphate concentrations. This response indicates a good mixing of event water (tracer) with pre-event water (groundwater). The maximum contribution of the artificial rainwater was up to 50–95% of the total

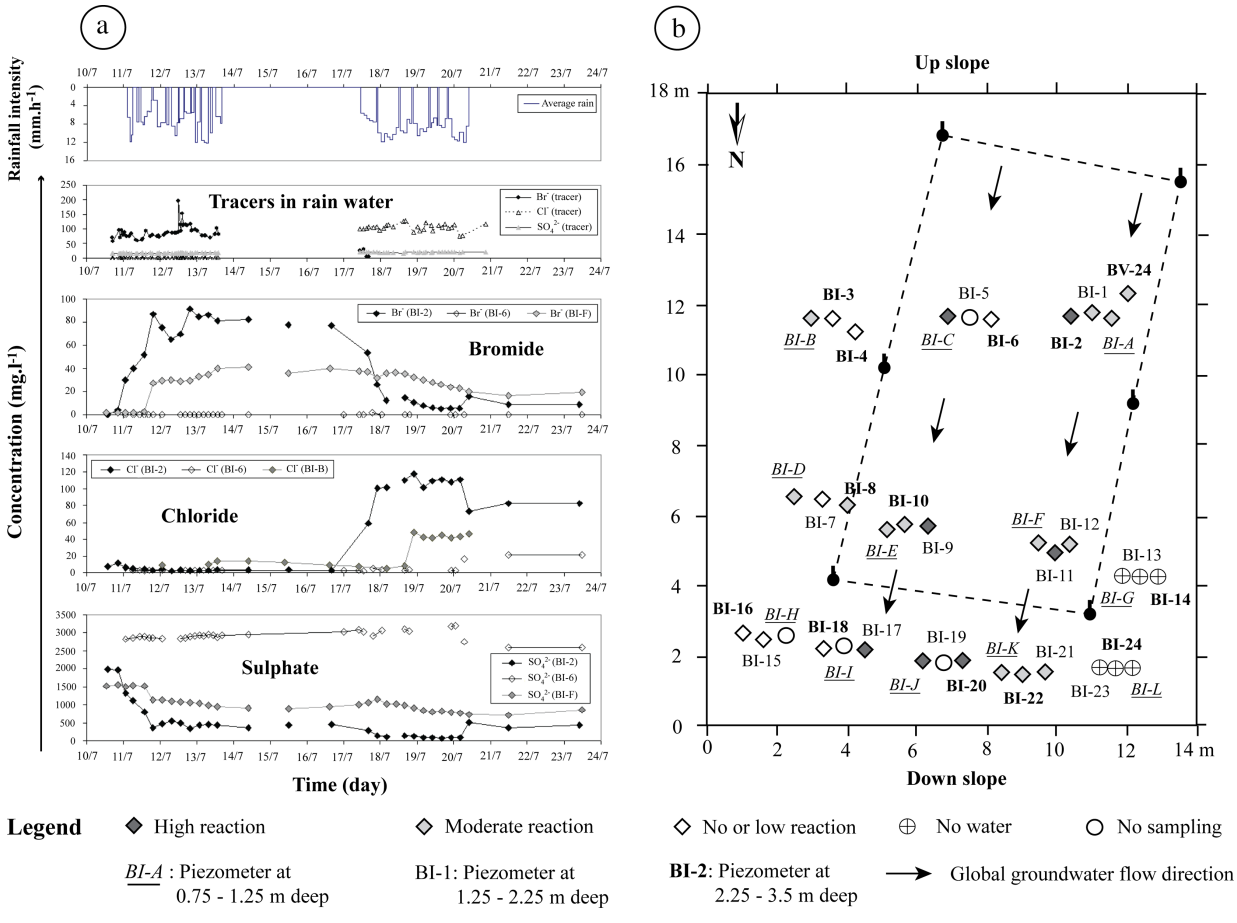

Figure 8. Observed hydrochemical changes in water quality during the rain experiment

Copyright © 2011 John Wiley & Sons, Ltd.

flow (ratio of maximum observed tracers' concentration in groundwater and average artificial rainwater concentration; the pre-event concentrations of Br^- and Cl^- are zero);

- a moderate response in BI-A, B, D, E, F, K, 1, 8, 10, 12, 21, 22, BV-24, which can be attributed to an increase of concentrations of bromide and chloride in the range of 20–60 mg l^{-1} and only a slight dilution of sulphate. This indicates a moderate mixing of event water (tracer) with pre-event water (groundwater). The event water contribution is of 15–50% of the total flow.
- no or limited response was detected in piezometers BI-3, 4, 6, 7, 15, 16 and 18 where the concentration of bromide and chloride remained low (<20 mg l^{-1}). This indicates a low amount of mixing of tracer with groundwater, in the order of less than 15% of rain water contribution.

Comparing the hydrological observations with the hydrochemical changes (Figures 4 and 8) illustrates that the moderate response coincides with an attenuated input and output (BI-A and BI-8) and that the high responses take place simultaneously with the fast input–output systems. Opposite however, piezometers BI-6 and BI-18 show a relatively fast input and output hydrological response and low tracer concentrations. This can be explained by water pressure (piston flow mechanism). This effect cannot be observed with just hydrological monitoring, and therefore underlines the importance of chemical observations.

Looking closely to the spatial distribution of the hydrochemical information (Figure 8b), it can be observed that:

- there is no relationship between the observed superficial fissure characteristics and tracer reaction, except for the shallow piezometers (BI-C and BI-B) in the south-east corner of the experimental plot. The piezometer BI-C (located inside the plot) has a high tracer response and the piezometer BI-B (located outside the plot) shows a moderate tracer response. This indicates a possible hydrological and hydrochemical connection between the two piezometers;
- there is no clear relationship between the depth of the piezometers and the tracer response. High tracer concentrations were found at different depths (1, 2 and 3 m), indicating fast preferential flow. Figure 8 indicates that moderate to high concentrations in Br^- and Cl^- were measured in shallow piezometers. A systematic impact of the applied rainwater was observed at low depths.

Figure 9 presents the comparison between the depth of the piezometer, the permeability, the measured groundwater level and the chemical characteristics.

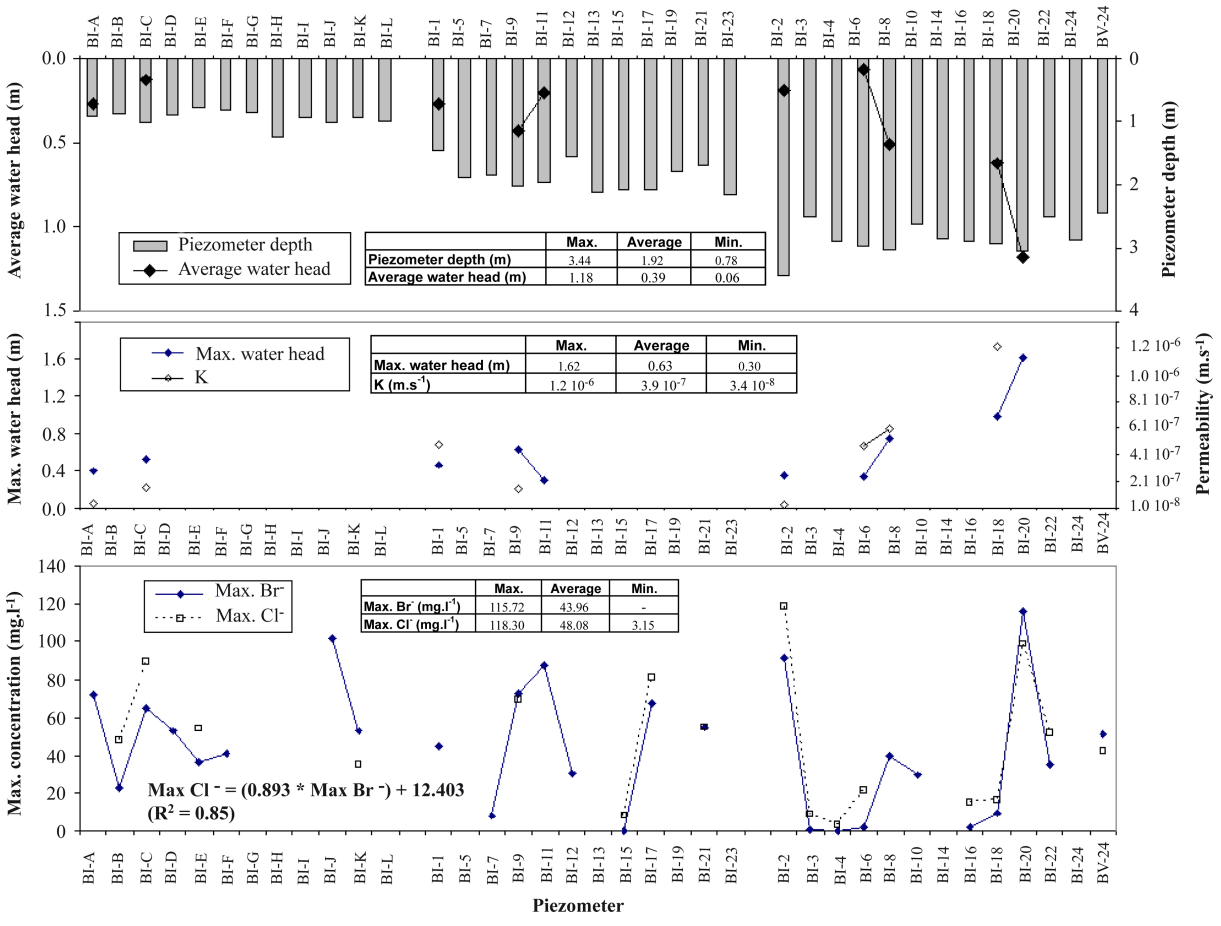

Figure 9. Relationship between the depth of the piezometer, the permeabilty, the measured groundwater level and the hydrochemical characteristics

Copyright © 2011 John Wiley & Sons, Ltd.

The maximum concentrations of bromide and chloride are strongly correlated ($R^2 = 0{\cdot}85$). This indicates that no significant modification in the soil structure and flow paths occurred inside the experimental plot between the first and second experiment. However, no correlation was found between the tracer concentration (Br^- and Cl^-), the permeability, the water level or the depth of the piezometer. This can quite be expected in a soil with such a high degree of heterogeneity.

Water and chemical budgets

The water budget was calculated over the period 10–23 July 2007 using:

$$V_{AR} = V_{RO} + \Delta V_{GWF} + E + \Delta S_s + \Delta S_u \quad (1)$$

where V_{AR} is the volume of artificial rain; V_{RO} is the volume of surface run-off; ΔV_{GWF} is the volume difference of groundwater in- and outflow; E is the volume of evaporated water; ΔS_s is the volume change of the saturated zone storage and ΔS_u is the volume change of the unsaturated zone storage.

The water budget equation is written for steady flow conditions prior to the experiment. Groundwater flow variation downstream was only due to artificial rainfall over the experimental plot.

The equation used to estimate the artificial tracers (Br^- and Cl^-) mass balance is given by:

$$M_{AR} = M_{RO} + M_{\Delta GWF} + M_{\Delta Ss} + M_{\Delta Su} \quad (2)$$

where M_{AR} is the tracer mass (Br^- or Cl^-) within the artificial rain; M_{RO} is the tracer mass in the surface water; $M_{\Delta GWF}$ is the tracer mass transferred groundwater between in- and outflow; $M_{\Delta S_s}$ is the tracer mass variation depending on the storage change in the saturated zone and $M_{\Delta S_u}$ is the tracer mass variation depending on the storage change in the unsaturated zone.

The bromide and chloride masses were calculated from the chemical measurements and water volume, according to the following equation:

$$M = \int_1^n C \times V \quad (3)$$

where M is the mass (mg); C is the concentration of Br^- or Cl^- in the water (mg l^{-1}); V is the volume of water (l); n is the number of chemical observations (the observations were carried out with 1, 3, 6 and 24 h time interval and over the period 10–23 July 2007; Figure 3).

Figure 10 indicates run-off as the most significant water balance term (81·4%) whereas only 16·6% of the rain infiltrated into the soil. The water balance indicates an overestimation of the outgoing water volume by 5·8%.

For the tracer mass balances, an underestimation of 0·3 kg (5·8%) was found for the bromide of 2·25 kg (25·2%) for the chloride. Basically, nearly all bromide applied during the rainfall experiment was flushed out. The loss of chloride is quite significant but can be explained because the chloride was only used in the second experiment and consequently was not totally flushed out at the end of the simulation. Overall, it can

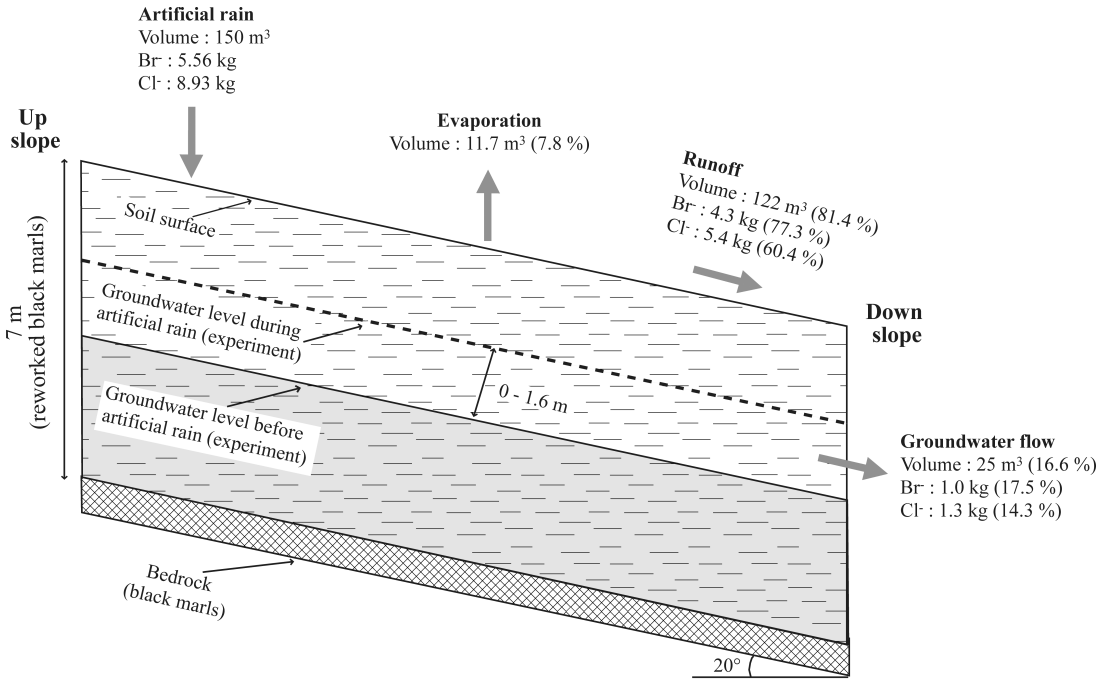

Water & chemical absolute balance error (out - in)			Water & chemical relative balance error (out - in)		
Water volume (m^3)	Br^- (kg)	Cl^- (kg)	Water volume (%)	Br^- (%)	Cl^- (%)
8.7	-0.3	-2.3	5.8	-5.3	-25.2

Figure 10. Water and tracers mass balances for the experiment over the period 10–23 July 2007

Copyright © 2011 John Wiley & Sons, Ltd.

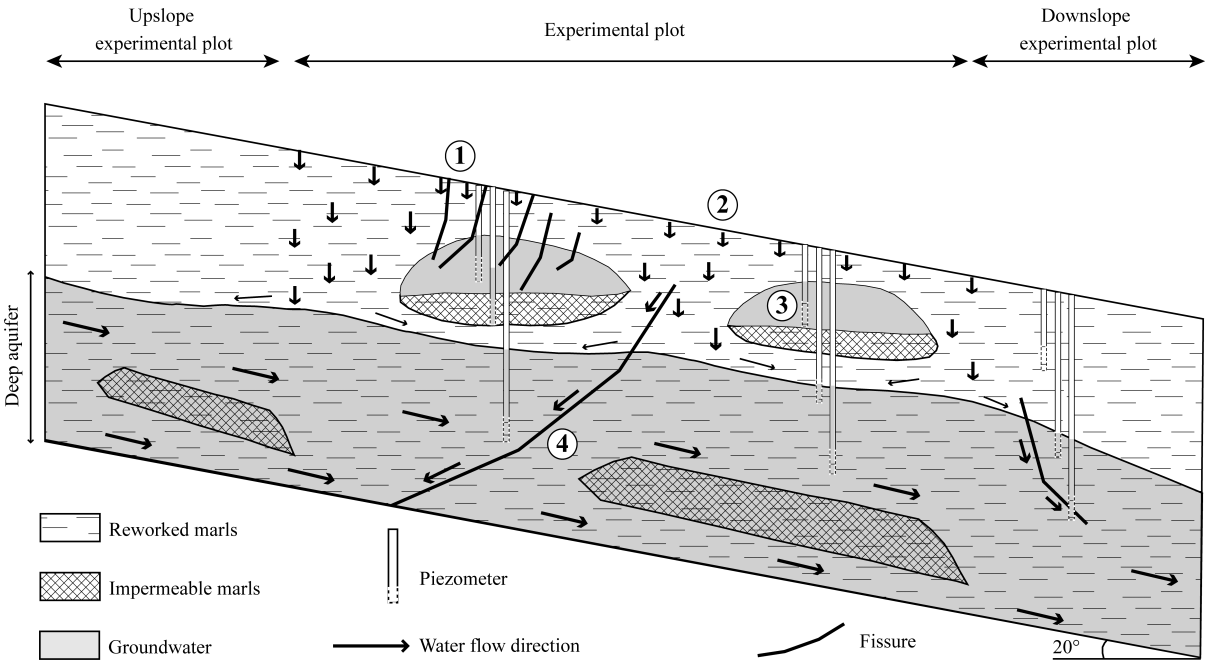

Figure 11. Conceptual model of subsurface water flow paths in the Super-Sauze mudslide. (1) Preferential infiltration; (2) Soil matrix infiltration; (3) Perched water bodies preventing deeper pore water pressure build-up; (4) Lateral preferential flow draining the groundwater system

be concluded that all major fluxes and stocks of water and chemical elements are measured and that significant losses or gains of water are unlikely.

A conceptual model of the subsurface water flow

The results outline that the hydrodynamic and hydrochemical changes are very large and could not be inferred from surface area characteristics. This experiment shows the predominance of vertical flow leading to high storage capacity, to the development of local perched water tables and to the fast deep transversal transfer of water according to the fissure network and subsurface topography. Figure 11 gives a conceptual model of the water pathways as encountered within the experimental plot. The rain infiltrates into the topsoil both through the soil matrix and preferential flow paths. In places, some impermeable blocks of unweathered black marls prevent the vertical percolation resulting in small perched water bodies. The water flow in the deeper groundwater body follows the overall slope gradient (20°). However, discontinuities such as fissures or macroporosity will influence the exact direction of the water flow.

The fact that fissures increases vertical infiltration is a well-established insight in slope hydrology research. Our experimental data suggest a double porosity system combined with highly irregular pore water pressure field in the landslide body. They clearly outline the extend of heterogeneity of the pore water pressure distribution built up because of the (temporal) development of local perched water bodies and because of the huge lateral drainage capacity within a landslide body. These latter two aspects are often neglected in the model approach, i.e. enhanced surface infiltration is followed by relatively homogeneous pore pressure built up and lateral Darcian matrix water flow (Haneberg, 1991; Angeli *et al*., 1998; Bogaard, 2001; Malet *et al*., 2005b).

In hillslope hydrology, research aiming at the understanding and quantification of discharge generation processes from hillslopes and the emerging discharge processes in heterogeneous soils are now well established (Onda *et al*., 2004; Uchida *et al*., 2005; Tromp-van Meerveld and McDonnell, 2006; Weiler and Mcdonnell, 2007). Also, the influence of subsurface topography and water flow heterogeneity underneath a soil layer has been reported several times to be very important (Wilson and Dietrich, 1987; Johnson and Sitar, 1990; Tromp-van Meerveld and McDonnell, 2006). Additionally, in some landslide studies, the draining influence of fissures on the decrease of the pore water pressure has been suggested, as well as the impact of rapid access to the lower groundwater system on the triggering frequency and response time (McDonnell, 1990; Reid and Iverson, 1992; Van Asch *et al*., 1999; Uchida *et al*., 2001; Binet *et al*., 2007). The understanding of hydrological behaviour of hillslopes and the results of our experiment point out that landslides are subject to heterogeneous pore water pressure built-up which influences the overall stability and movement of landslides.

CONCLUSION

A quite complex hydrological conceptual model of the Super-Sauze mudslide area is proposed with high infiltration capacity, fast recharge of the (deeper) groundwater system but also with localized distribution of perched saturated zones. This study confirmed the relevance of tracing tests to investigate hydrodynamic processes in heterogeneous unstable media. Deep groundwater level

Copyright © 2011 John Wiley & Sons, Ltd.

variations were explained by preferential flow processes (contribution of new water) and pressure transfer (piston effect). Depending on the observation point, direct recharge water reached draining zones or conversely was durably stored. The knowledge that pore water pressure distribution presents such a large degree of heterogeneity should be incorporated within slope stability assessment. Unfortunately, most of the time, field observations are too limited to perceive such complex lateral subsurface flow patterns like dead end fissures, fast outflows or unsaturated wedges underneath enclosed low permeable blocks within the landslide body. This point is of huge importance as it advises against the unsuitable use of any forecasting tools simply based on surface observation. Here research attention should turn towards the development of innovative experimental means to investigate the emerging hydrological behaviour of preferential flow paths and their organisation within the soil.

ACKNOWLEDGEMENTS

This work has been supported by two French-funded projects (ANR ECOU-PREF 'Ecoulements préférentiels dans les versants marneux' and ANR TRIGGERLAND 'TRIGGERing mechanisms of LANDslides: analysis and modelling', and by the European Commission within the Marie Curie Research and Training Network 'Mountain Risks'. The authors would like to thank Julien Travelletti, Vincent Allègre (*CNRS/University of Strasbourg*), Olivier Maquaire (*University of Caen-Basse-Normandie*) for their support during the field experiment, Roland Simler (University of Avignon) for his contribution to the chemical analysis of waters and the anonymous reviewers for their constructive comments.

REFERENCES

Aboukhaled A, Alfaro A, Smith M. 1982. Lysimeters. FAO Irrigation Drainage Paper No. 39, FAO, Rome, Italy, 68 p.

Allaire SE, Gupta SC, Nieber J, Moncrief JF. 2002. Role of macropore continuity and tortuosity on solute transport in soils: 1. Effects of initial and boundary conditions. *Journal of Contaminant Hydrology* **58**: 299–321.

Allaire-Leung SE, Gupta SC, Moncrief JF. 2000. Water and solute movement in soil as influenced by macropore characteristics—1. Macropore continuity. *Journal of Contaminant Hydrology* **41**(3–4): 283–301.

Angeli MG, Buma J, Gasparetto P, Pasuto A. 1998. A combined hillslope hydrology/stability model for low gradient clay slopes in the Italian Dolomites,. *Engineering Geology* **49**: 1–13.

Binet S, Jomard H, Lebourg T, Guglielmi Y, Tric E, Bertrand C, Mudry J. 2006. Experimental analysis of groundwater flow through a landslide slip surface using natural and artificial water chemical tracers,. *Hydrological Processes* **21**(25): 3463–3472.

Binet S, Mudry J, Scavia C, Campus S, Bertrand C, Guglielmi Y. 2007. In situ characterization of flows in a fractured unstable slope. *Geomorphology* **86**(15): 193–203.

Boast CW, Robertson TM. 1982. A micro-lysimeter method for determining evaporation from bare soil: Description and laboratory evaluation. *Soil Science Society of America Journal* **46**: 689–696.

Bogaard TA. 2001. *Analysis of hydrological processes in unstable clayey slopes*. Amsterdam/Utrecht KNAG/Faculteit Ruimtelijke Wetenschappen, Universiteit Utrecht. Doctoral thesis, Netherlands Geographical Studies, 287 p.

Bogaard TA, Buma JT, Klawer CJM. 2004. Testing the potential of geochemical techniques for identifying hydrological systems within landslides in partly weathered marls. *Geomorphology* **58**: 323–338.

Bouwer H, Rice RC. 1976. A Slug test for determining hydraulic conductivity of unconfined aquifers with completely or partially penetrating wells. *Water Ressources Research* **12**(3): 423–428.

Cras A, Marc V, Travi Y. 2007. Hydrological behaviour of submediterranean alpine headwater steams in a badland environment. *Journal of Hydrology* **339**(3–4): 130–144.

De Montety V, Marc V, Emblanch C, Malet JP, Bertrand C, Maquaire O, Bogaard TA. 2007. Identifying the origin of groundwater and flow processes in complex landslides affecting black marls: insights from a hydrochemical survey. *Earth Surface Processes and Landforms* **32**: 32–48.

Einsiedl F. 2005. Flow system dynamics and water storage of a fissured-porous karst aquifer characterized by artificial and environmental tracers. *Journal of Hydrology* **312**(1–4): 312–321.

Gerke HH, van Genuchten MTh. 1993. A dual-porosity model for simulating the preferential movement of water and solutes in structured porous media. *Water Resources Research* **29**: 305–319.

Grandjean G, Pennetier C, Bitri A, Meric O, Malet JP. 2006. Characterization of the internal structure and the hydric state of clayey-marly landslides through geophysical tomography: example of the Super-Sauze earthflow (French South Alps). *Comptes Rendus Geoscience* **338**(9): 587–595.

Gwo JP, Jardine PM, Wilson GV, Yeh GT. 1995. A multiple-pore-region concept to modeling mass transfer in subsurface media. *Journal of Hydrology* **164**: 217–237.

Haneberg WC. 1991. Pore pressure diffusion and the hydrologic response of nearly saturated, thin landslide deposits to rainfall. *Journal of Geology* **99**(8): 886–892.

Hirotaka O, Yasuhiko O, Gen F, Yoichi O, Takuro M, Toshiaki S, Tomomi T, Kyoji S. 2004. A fluidized landslide on a natural slope by artificial rainfall. *Landslides* **1**: 211–219.

Hutson JL, Wagenet RJ. 1995. A multiregion model describing water flow and solute transport in heterogeneous soils. *Soil Science Society of America Journal* **59**: 743–751.

Jarvis NJ. 1994. *The MACRO Model (Version 3.1). Technical Description and Sample Simulations*. Reports and Dissertations 19. Department of Soil Science, Swedish University of Agricultural Science, Uppsala, Sweden, 51 p.

Javaux M, Vanclooster M. 2006. Scale-dependency of the hydraulic properties of a variably saturated sandy subsoil. *Journal of Hydrology* **327**(3–4): 376–388.

Johnson KA, Sitar N. 1990. Hydrologic conditions leading to debris-flow initiation. *Canadian Geotechnical Journal* **27**: 789–801.

Kabeya N, Katsuyama M, Kawasaki M, Ohte N, Sugimoto A. 2007. Estimation of mean residence times of subsurface waters using seasonal variation in deuterium excess in a small headwater catchment in Japan. *Hydrological Processes* **21**(3): 308–322.

Lacube J, Durville JL. 1989. Un essai de fichier informatique sur les mouvements de terrain. *Bulletin de Liaison des Laboratoires des Ponts et Chaussées* **161**: 86–89.

Larsbo M, Jarvis N. 2006. Information content of measurements from tracer microlysimeter experiments designed for parameter identification in dual-permeability models. *Journal of Hydrology* **325**(1–4): 273–287.

Liu HH, Zhang R, Bodvarsson GS. 2005. An active region model for capturing fractal flow patterns in unsaturated soils: model development. *Journal of Contaminant Hydrology* **80**: 18–30.

Malet JP. 2003. *Les 'glissements de type écoulement' dans les marnes noires des Alpes du Sud. Morphologie, fonctionnement et modélisation hydro-mécanique*. Doctoral thesis, University Louis Pasteur, Strasbourg, 362 p.

Malet JP, Auzet AV, Maquaire O, Ambroise B, Descroix L, Esteves M, Vandervaere JP, Truchet E. 2003. Soil surface characteristics influence on infiltration in black marls: application to the Super-Sauze earthflow (southern Alps, France). *Earth Surface Processes and Landforms* **28**(5): 547–564.

Malet JP, Laigle D, Remaître A, Maquaire O. 2005a. Triggering conditions and mobility of debris flows associated to complex earthflows. *Geomorphology* **66**: 215–235.

Malet JP, Van Asch TWJ, Van Beek R, Maquaire O. 2005b. Forecasting the behaviour of complex landslides with a spatially distributed hydrological model. *Natural Hazards and Earth System Science* **5**(1): 71–85.

Mali N, Urbanc J, Leis A. 2007. Tracing of water movement through the unsaturated zone of a coarse gravel aquifer by means of dye and deuterated water. *Environmental Geology* **51**(8): 1401–1412.

Copyright © 2011 John Wiley & Sons, Ltd.

Mcdonnell JJ. 1990. The influence of macropores on debris flow initiation. *Quarterly Journal of Engineering Geology* **23**(4): 325–331.

Onda Y, Tsujimura M, Tabuchi H. 2004. The role of subsurface water flow paths on hillslope hydrological processes, landslides and landform development in steep mountains of Japan. *Hydrological Processes* **18**(4): 637–650.

Pruess K, Wang JSY. 1987. Numerical modeling of isothermal and non-isothermal flow in unsaturated fractured rock—a review. In *Flow and Transport through Unsaturated Fractured Rock*, *Geophysics Monograph*, 42: Evans DD, Nicholson TJ (eds). 11–22.

Reid ME, Iverson RM. 1992. Gravity-driven groundwater flow and slope failure potential 2. Effects of slope morphology, material properties, and hydraulic heterogeneity. *Water Resources Research* **28**(3): 939–950.

Schoen R, Gaudet JP, Bariac T. 1999a. Preferential flow and solute transport in a large lysimeter, under controlled boundary conditions. *Journal of Hydrology* **215**: 70–81.

Schoen R, Gaudet JP, Elrick DE. 1999b. Modelling of solute transport in a large undisturbed lysimeter, during steady-state water flux. *Journal of Hydrology* **215**: 82–93.

Stumpp C, Maloszewski P, Stichler W, Maciejewski S. 2007. Quantification of the heterogeneity of the unsaturated zone based on environmental deuterium observed in lysimeter experiments. *Hydrological Sciences Journal/Journal des Sciences Hydrologiques* **52**(4): 748–762.

Travelletti J, Oppikofer T, Delacourt C, Malet JP, Jaboyedoff M. 2008. *Monitoring landslide displacements during a controlled rain experiment using a long-range terrestrial laser scanning (TLS)*. In *ISPRS—International Archives of the Photogrammetry, Remote Sensing and Spatial Information Sciences*, vol. XXXVII (Part B5), Beijing, China, 485–490.

Tromp-van Meerveld HJ, McDonnell JJ. 2006. Threshold relations in subsurface stormflow: 1. A 147-storm analysis of the Panola hillslope. *Water Resources Research* **42**: W02410, DOI:10.1029/2004WR003778.

Uchida T. 2004. Clarifying the role of pipe flow on shallow landslide initiation. *Hydological Processes* **18**(2): 375–378.

Uchida T, Kosugi K, Mizuyama T. 2001. Effects of pipeflow on hydrological process and its relation to landslide: a review of pipeflow studies in forested headwater catchments. *Hydological Processes* **15**: 2151–2174.

Uchida T, Tromp-Van Meerveld I, Mcdonnell JJ. 2005. The role of lateral pipe flow in hillslope runoff response: An intercomparison of non-linear hillslope response. *Journal of Hydrology* **311**(1–4): 117–133.

Van Asch TWJ, Buma J, Van Beek LPH. 1999. A view on some hydrological triggering systems in landslides. *Geomorphology* **30**: 25–32.

van Genuchten MTh, Wierenga PJ. 1976. Mass transfer studies in sorbing porous media. I. Analytical solutions. *Soil Science Society of America Journal* **40**: 473–481.

Viville D, Ladouche B, Bariac T. 2007. Isotope hydrological study of mean transit time in the granitic Strengbach catchment (Vosges massif, France): application of the FlowPC model with modified input function. *Hydological Processes* **20**(8): 1737–1751.

Weiler M, Mcdonnell JJ. 2007. Conceptualizing lateral preferential flow and flow networks and simulating the effects on gauged and ungauged hillslopes. *Water Resources Research* **43**(3): W03403.

Wilson CJ, Dietrich WE. 1987. *The contribution of bedrock groundwater flow to storm runoff and high pore pressure development in hollows*. In *Proceedings of the Corvallis Symposium: Erosion and Sedimentation in the Pacific Rim*. IAHS Publications 165: 49–59.

Copyright © 2011 John Wiley & Sons, Ltd.